


Electrolyte structure near electrodes with molecular-size roughnessTimur Aslyamov ^{*}*Center for Design, Manufacturing and Materials, Skolkovo Institute of Science and Technology, Bolshoy Boulevard 30, bld. 1, Moscow, 121205 Russia*Konstantin Sinkov [†]*Schlumberger Moscow Research, Leningradskoe shosse 16A/3, Moscow, 125171 Russia*

Iskander Akhatov

Center for Design, Manufacturing and Materials, Skolkovo Institute of Science and Technology, Bolshoy Boulevard 30 bld. 1, Moscow, 121205 Russia

(Received 24 February 2021; accepted 1 June 2021; published 22 June 2021)

Understanding electrodes' surface morphology influence on ions' distribution is essential for designing supercapacitors with enhanced energy density characteristics. We develop a model for the structure of electrolytes near the rough surface of electrodes. The model describes an effective electrostatic field's increase and associated intensification of ions' spatial separation at the electrode-electrolyte interface. These adsorption-induced local electric and structure properties result in notably increased values and a sharpened form of the differential capacitance dependence on the applied potential. Such capacitance behavior is observed in many published simulations, and its description is beyond the capabilities of the established flat-electrodes theories. The proposed approach could extend the quantitatively verified models providing a new instrument of the electrode surface-parameter optimization for specific electrolytes.

DOI: [10.1103/PhysRevE.103.L060102](https://doi.org/10.1103/PhysRevE.103.L060102)

Supercapacitors have some of the best prospects of modern energy sources due to the outstanding charging and discharging times, extremely long life cycle, and ecology-friendly process of the charge storage [1]. Since supercapacitors store electrical energy using the ions' adsorption, the porous carbon materials with a high specific surface area (SSA) are used as popular electrodes [2–4]. Such materials exhibit wide pore size distribution dividing a large pore volume between micro- and mesoscales [5]. However, the vital experimental discovery of the capacitance increase inside subnanoporous electrodes [6] shows that not all pores contribute effectively to the capacity. Further experimental [7] and theoretical [8] studies demonstrated that the capacitance of the nanoporous electrodes is an oscillating function of the size of the pores with the largest value corresponding to pore's size comparable to the ion diameter. This anomalous enhancement of the capacity demands the dense packing of the identically charged ions in spite of the electrostatic repulsion. It was explained and simulated in [9,10] accounting for the polarization of the conductive pore boundaries which screens the electrostatic ion-ion interaction. These results show the importance of the molecular-size influence on the electrode-electrolyte interface storing the energy in the supercapacitor-based technologies. Thus, the molecular-scale surface roughness which is inherent for the carbons mesopores [11] could crucially influence the capacity properties.

The investigation of the morphology's influence on the electrical properties has a long history starting with the experiments with solid metal electrodes (see [12] for review). The first models were developed by Daikhin, Kornyshev, and Urbakh for the description of the diluted electrolytes near the electrodes with a weak roughness. The authors used perturbation theory for both the linear [13] and nonlinear [14] Poisson-Boltzmann equations. The electrostatic fields perturbed by the roughness have been shown to result in the increase of the capacity in comparison with the flat electrodes. The systematic molecular dynamic (MD) studies [15–20] demonstrated the enhanced capacitance for the carbon electrodes with the molecular-scale patterns on the surface. Very recently the importance of the morphology has been clearly illustrated by the experimental comparison of two porous carbon samples with almost equal SSA, porous size distribution, and composition but different surface roughness [21]. The measured capacitance of the material with higher roughness is more than 50% higher than the smoother electrode. Thus, the adoption of the nanosize pores is not the only direction to enhance the capacitance, another option is using electrodes with geometrically heterogeneous surfaces [22].

The differential capacitance (DC) C_d depending on the applied potential U is traditionally used as the main characteristic to quantify the geometrical influence on the electrostatic properties in the experiments [23,24] and simulations mentioned above. In the case of flat electrodes, Kornyshev [25] predicted that DC as a function of potential exhibits camel or bell shapes in the dependence on the electrolyte packing density. The extension of this mean-field model accounting for

^{*}t.aslyamov@skoltech.ru[†]sinkovk@gmail.com

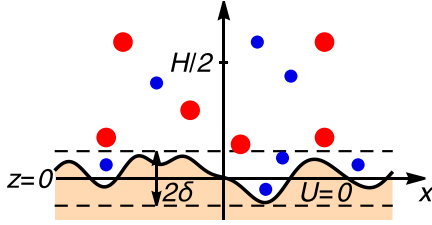


FIG. 1. The sketch illustrates the characteristic distribution of the asymmetric ions near a rough surface at positive applied potential.

intermolecular interactions [26] provides more realistic DC properties: a smoother form and reduced maximum values for the DC dependence on the potential. Also, a similar mean-field density functional was used to estimate the number ratio of the bounded (neutral clusters) and free states of the particles in the ionic liquids [27]. In the case of rough electrodes the computer simulations indicate a more complicated DC behavior; for example, the MD study [15] showed that the electrode surface's geometrical heterogeneity could alter the form of the ionic liquids' DC from the camel shape to bell shape. Also, in [16] the authors considered significantly rough surfaces which induce a sharper form of the DC and the existence of a larger number of peaks. Thus, to describe the rough surface influence on the DC the desired theory should extend the surface description beyond flat and curved geometries [25,28–30] and account for more realistic concentrate electrolyte properties than used in pioneering works [13,14]

In this work, we develop a mean-field model describing the electrolyte behavior near rough electrode surfaces. Here we focus on the ionic liquids [31] exhibiting the complex behavior of DC in the dependence of the surface roughness [20,22]. In order to demonstrate the influence of the electrode roughness on the DC properties more explicitly we consider a simple mean-field model [25] as a basis (the flat electrode limit). The mean-field models [25,26] describe the structureless “crowding” state only. Description of the well-structured “overscreening” demands models beyond mean field; see, for example, [32,33]. However, the oscillating charge behavior indicating the overscreening has been observed in experiments with atomically flat electrodes only [26]. Moreover, it is known from theory [34] and experiment [11] that surface heterogeneity destroys the well-structured adsorbent's layering. Therefore, as it has been previously noted [26] that the surface heterogeneity makes relatively simple mean-field models more appropriate for the description of the capacity behavior. Similarly to works [13,14] we use perturbation theory to obtain the boundary condition for the Poisson equation [35]. But unlike approaches in [13,14] we account for the local properties of the random surface to obtain the average ion distributions closing a system of the self-consistent equations.

In our model, the solid surface profile is the correlated Gauss process $z_s(x)$, where x is the coordinate in the lateral direction, and the standard deviation δ and the correlation length λ define the roughness in the normal direction and the characteristic lateral structure, respectively (see Fig. 1). We put the origin of the normal coordinate z so that the solid profile average equals zero $\overline{z_s(x)} = 0$. The standard deviation defines the vertical distribution of the solid media,

and the correlation properties correspond to the decreasing exponential function $\overline{z_s(x)z_s(x+t)} \sim e^{-|t|/\lambda}$. Therefore, the small λ induces the palisade of the solid peaks, and the large λ results in the formation of the sparse structure allowing the fluid molecules to penetrate into perturbed or rough region of the solid medium. Thus, to describe the ions molecules' behavior near rough surfaces, both normal δ and correlation λ parameters are crucial. Such a two-parametric random surface model provides height profiles mimicking the geometry of the real materials [36,37] and has a substantial advantage over deterministic well-structured geometries allowing description of randomly distributed surface-heterogeneity (defects and functional groups) [38,39].

The electrolyte fills the available space that results in the inhomogeneous density distributions of the ions mixture $\rho_i = \rho_i(x, z)$. Accounting for the applied potential U the electrostatic field $\psi = \psi(x, z)$ inside the pore is defined by the Poisson equation and the boundary conditions

$$\begin{aligned} \beta e \Delta \psi &= -4\pi \lambda_B q & \text{in } D, \\ \psi &= U & \text{at } \partial D, \end{aligned} \quad (1)$$

where $\beta = 1/k_B T$, k_B is the Boltzmann constant, T is the temperature, e is the electron charge, $\Delta = \partial_{xx} + \partial_{zz}$ is the 2D Laplace operator, $q = \sum_i Z_i \rho_i$, Z_i are the valencies, and $\lambda_B = \beta e^2 / (4\pi \epsilon \epsilon_0)$ is the Bjerrum length. The domain $D = \{x, z_s(x) < z < H/2\}$ is half-space of the pore of width H above rough surface $\partial D = \{x, z = z_s(x)\}$. We impose the zero field condition at the half width $\psi(H/2) = 0$ and, thus, consider sufficiently large pores.

Subdividing D into the (bulk) volume $D_v = \{x, \delta < z < H/2\}$ and the (near-)surface $D_s = \{x, -\delta < z < \delta\}$ domains and applying a perturbation procedure [35] involving matching expansions for the electrostatic potential and charge density with respect to $\epsilon = 2\delta/H \ll 1$ in D_v and D_s , we show (see the Supplemental Material [40], Sec. I) that the average electrostatic field $\overline{\psi} = \overline{\psi}(z)$ above a rough surface can be approximated with an error $O(\epsilon^2)$ by the piecewise solution

$$\overline{\psi} = \begin{cases} \overline{\psi}_v, & z \geq \delta \\ \overline{\psi}_s, & z < \delta. \end{cases}$$

Here the averaging is performed over the realizations of the Gauss random process with exponentially decaying lateral correlation representing the rough surface [see Eqs. (S10) and (S11) [40] for exact definitions via one- and two-point distribution functions]. The field in the volume domain $\overline{\psi}_v$ is given by solution of the following problem:

$$\begin{aligned} \beta e \partial_{zz} \overline{\psi}_v &= -4\pi \lambda_B \overline{q}, & z \geq \delta, \\ \overline{\psi}_v &= U + \delta \partial_z \overline{\psi}_v, & z = \delta, \end{aligned} \quad (2)$$

and the field in the surface domain $\overline{\psi}_s$ is given by

$$\overline{\psi}_s = U + z \partial_z \overline{\psi}_v|_{z=\delta}, \quad z < \delta. \quad (3)$$

$\overline{\psi}_s$ is linear in z and naturally equals to the applied voltage at the apparent boundary of the pore $z = 0$. The slope of the $\overline{\psi}_s$ dependency on z is defined by the gradient of the electrostatic field $\overline{\psi}_v$ at the boundary $z = \delta$ such that $\overline{\psi}$ is smooth in the entire domain. The problem (2) for the average field $\overline{\psi}_v$ is decoupled from the surface domain. Thus, the density distribution in the inner region is needed only

to determine the electrostatic field in the entire pore. However, the density in the surface domain crucially influences the charge and capacitance properties. The total charge is defined by the summation of the volume and surface regions $Q = Q_s + Q_v$, where the cumulative contributions are defined from the integrals $Q_s = \int_{-\delta}^{\delta} e\bar{q}(z) dz$ and $Q_v = \int_{\delta}^{H/2} \sum e\bar{q}(z) dz$.

Besides the electrostatic forces, the ions interact with the solid boundaries via Lennard-Jones potential. We model this interaction as hard wall repulsion and consider the ionic liquid as hard spheres mixture [41]. In the electrodes with flat surfaces, the minimal distance between ions and solid boundaries is defined by the hard sphere radii $d_i/2$. This behavior contrasts with the molecules distributions near rough surfaces that allow ions to penetrate into the rough region of solid medium. Therefore, the function of the ions' spatial distribution starts from some points $z_i < d_i/2$. This starting point z_i may be negative for extremely rough surfaces and tends to the hard wall value $d_i/2$ as the roughness becomes insignificant. Considering the rough surface as the Gauss correlated process the contact conditions can be calculated as functions of the relative roughness parameters $z_i(\delta/d_i, \lambda/d_i)$ [40]. The details of the dependence of the ions' penetration into solid media on the surface roughness and the diameter of molecules can be found in [40], Sec. II. In comparison with the flat surface, the roughness results in the region which is filled by both ions and solid molecules, but at the same time, the vertical distribution of the solid media decreases the space permitted for the ions. It can be accounted by excluding the ratio of solid media at each level z from the whole covered surface, then the permitted surface area as a function of z has the following form:

$$S(z) = S_0 s(z) = S_0 \left(1 - \frac{1}{2} \operatorname{erfc} \frac{z}{\sqrt{2}\delta} \right), \quad (4)$$

where S_0 is the area of the surface projection on the lateral plane. Expression (4) depends on the standard deviation only and defines the vertical impact of the roughness (see derivation in [40], Sec. II).

To describe the electrolyte near rough surfaces we take into account the average properties of the random rough surface: the averaged electrostatic field, the modified configuration volume, and the hard sphere interaction with the rough surface. We account for these effects in terms of the Helmholtz free energy potential F defined in the volume free from solid media $\int S(z) dz$:

$$F[\{\bar{\rho}_i\}] = \int S(z) dz \sum_i [U_i^{\text{ext}}(z) + \bar{\psi}(z)Z_i] \bar{\rho}_i(z) + F^{HS}, \quad (5)$$

where $U_i^{\text{ext}}(z)$ is the hard boundary potential, and F^{HS} is the contribution from hard spheres interaction. The equilibrium condition defines the chemical potentials $\mu_i = \frac{1}{S(z)} \frac{\delta F[\{\bar{\rho}_i\}]}{\delta \bar{\rho}_i}$, which are constant across the volume. As one can see from the detailed calculations in [40], Sec. III, the density distributions have the following form:

$$\bar{\rho}_i(z) = s(z)\theta(z - z_i)\rho_i^0 \frac{e^{-Z_i\beta e\bar{\psi}}}{1 - \sum_i \gamma_i + \sum_i \gamma_i e^{-Z_i\beta e\bar{\psi}}}, \quad (6)$$

where ρ_i^0 is the bulk density describing the component far enough from the surface, and $\gamma_i = v_i\rho_i^0$ are the model parameters showing the packing density of the fluids, where

$v_i = \pi d_i^3/6$ is the ions volume. It is worth noting that in the case of $z_i = 0$, $\rho_i^0 = \rho^0$ and $v_i = v$ the result (6) agrees with [25] for $\gamma = \sum_i v_i\rho_i^0$.

In contrast with the perturbation theory for the Poisson-Boltzmann equation [13,14] where the calculation of the electrostatic field corrections up to the second order in roughness has been required to determine the first nonvanishing correction to capacity, we keep only first-order terms while deriving the system (2) and (3) (see [40], Sec. I). A notable result of our calculations, illustrated below, is that in the case of nonequal minimal distances between the ions' centers and solid surface z_i , the first-order theory is sufficient to reproduce nontrivial contribution of roughness to differential capacity.

We consider the binary mixture of the hard sphere molecules with the opposite charges $Z_1 = -Z_2 = 1$ and nonequal diameters $d_1 \neq d_2$. In the absence of applied voltage, the mixture is electrically neutral and composition bulk densities are equal $\rho^0 = \rho_i^0$. The following dimensionless variables are introduced: $U^* = eU/k_B T$, $z^* = z/d_m$, $H^* = H/d_m$, $Q^* = Q/e\rho^0 d_m$, $\lambda_B^* = \lambda_B d_m^2 \rho^0$, where $d_m = \min(d_1, d_2)$ is the molecular diameter of the smallest component.

First, we investigate the case of a flat pore wall surface $\delta = 0$. The minimal distances between the flat surface and the center of ion are equal to ions' radii $z_i^0 = d_i/2$. Figure 2(a) shows the dimensionless DC $C_d = \partial Q^*/\partial U^*$ as a function of the potential U^* for the case of cations larger than anions. Similarly to the model [25], the high potential limit of the DC is $C_d \sim 1/\sqrt{\gamma_2|U|}$ and $C_d \sim 1/\sqrt{\gamma_1|U|}$ for positive and negative U , respectively. Since composition bulk densities $\rho^0 = \rho_i^0$ are equal for $Z_1 = -Z_2 = 1$, the ratio of right and left wings of C_d shown in Fig. 2(a) is defined by the ions sizes as $(\gamma_1/\gamma_2)^{1/2} = (d_1/d_2)^{3/2}$. As one can see from Fig. 2(a) the DC at negative potential, where a contribution of the larger cations to charge dominates, is lower than at a positive one. Such asymmetric behavior agrees with published data of MD simulations [42] shown in Fig. 2(a). Also, Fig. 2(a) demonstrates that the number of capacitance maxima depends on the bulk density ρ^0 . The curves corresponding to sufficiently low γ_i exhibit two maximum points, the sharp and diffuse peaks at regions of small and large ions prevailing contribution to the total charge, respectively.

The roughness induces more striking changes in the capacitance properties. To isolate the impact from the surface geometry, we considered a slightly asymmetrical electrolyte with the molecular diameter ratio $d_2 = 4/3d_1$. The characteristic examples of the calculated electrostatic fields and ion distributions as functions of the coordinate z are shown in Fig. 2(b). As one can see, the considered parameters allow us to apply our approach for pores larger than six molecular diameters, that for ionic liquids corresponds to mesopores $H > 2$ nm. The rough surface allows molecules to reach the surface region ($z < \delta$), where the electrostatic field is defined by (3). Inside the surface region, the absolute value of electrostatic field $|\psi^*(z)|$ locally increases [see Fig. 2(b)] due to the sharp decrease of the permitted surface $S(z)$. Such potential behavior crucially influences the ion distributions improving the spatial separations of the co- and counterions. Figure 2(b) shows that the counterion cumulative effect from the surface region becomes overwhelming as the applied potential increases, while the electrolyte behavior in the volume domain

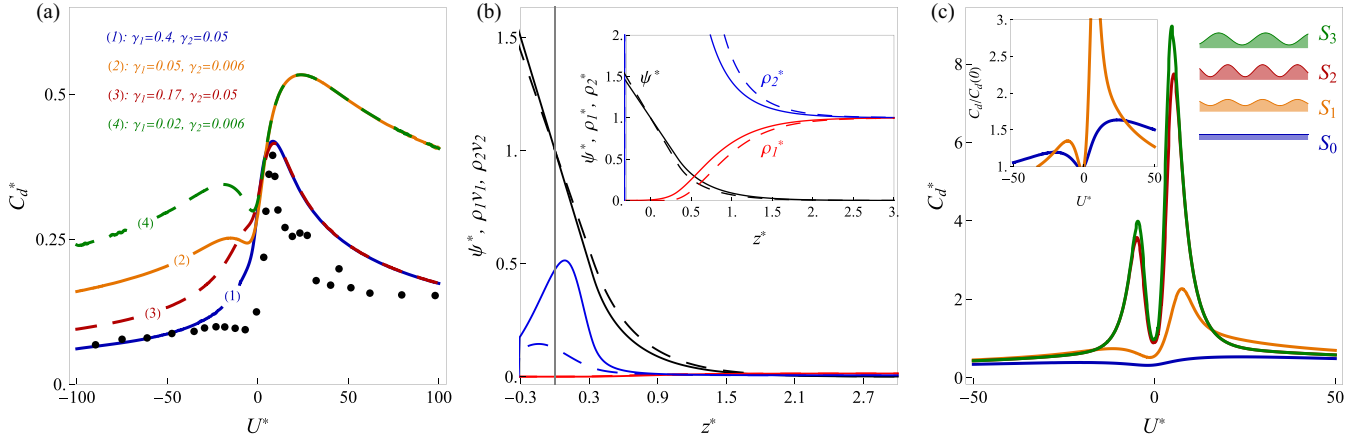


FIG. 2. (a) Flat electrode DC of ions mixtures with $d_1 = 2d_2$ (solid lines) and $d_1 = 1.5d_2$ (dashed lines). MD simulations results [42] also shown for reference (disks). (b) The relative electrostatic potential ψ^*/U^* (black), cations $\rho_1 v_1$ (red), and anions $\rho_2 v_2$ (blue) packing density distributions at two applied potentials $U^* = 4$ (solid lines) and $U^* = 8$ (dashed lines). Molecular diameter ratio $d_1 = 4/3d_2$, $\gamma_1 = 0.014$, $\gamma_2 = 0.006$, $\lambda_B^* = 0.25$. Surface parameters ($\delta^* = 0.33$, $\lambda^* = 1.66$, $z_1^* = -0.17$, $z_2^* = -0.31$) correspond to the surface S_3 shown in Fig. 2(c). Inset shows the detailed distribution inside the inner region using normalized density $\rho_i^* = \rho_i/\rho_0$. (c) The DC for the a binary mixture with $d_1 = 4/3d_2$ with $\gamma_1 = 0.014$, $\gamma_2 = 0.006$, $\lambda_B^* = 0.25$ near the various surface geometries: from flat S_0 to significantly rough S_3 (the surface parameters can be found in the Supplemental Material [40], Sec. 2). Inset shows the larger scale of DC for flat S_0 and slightly rough S_1 surfaces.

($z > \delta$) remains almost unperturbed. The contribution of Q_s to the total charge is notable and significantly improves the capacity properties. Therefore, the surface roughness induces the enhancement of the integral capacity that is in agreement with published simulations, for example, [16,22] and recent experiment [21]. Moreover, in [16] the capacitance enhancement also has been attributed to the local increase of the electrostatic field near a rough surface and its influence on the co- and counterion distribution inside the electrode-electrolyte interface (cumulative density).

To describe the total charge dependency on the applied potential, we calculated the DC C_d for the rough electrodes. Figure 2(c) shows our results for various surface morphology varying from flat to significantly rough. As one can see from Fig. 2(c) the roughness notably increases the capacitance and, in particular, the values of $C_d(U)$ maxima. Indeed, the quantitative comparison of the results from Fig. 2(c) shows that the flat DC is almost constant, while the surfaces with the higher roughness exhibit larger C_d values and extremely sharp peaks. Such DC behavior agrees with the observations from MD simulations [15,16] for ionic liquids inside rough electrodes. The calculated DC curves from Fig. 2(c) conserve the number of peaks, while the MD simulations [15,16] predict the roughness-induced appearance and disappearance of the DC curves maxima. The results of [16] allow us to explain this discrepancy. The authors of [16] demonstrated that the cumulative center-of-mass ion densities describe the DC curve at a finite range of the potential containing only two peaks, and the formation of the additional peaks is related to the steric effect of the ions spatial orientations. Therefore, our model's application is limited by the influences of the electrostatic potential and ion distributions of center of mass near rough electrodes. However, the roughness-induced transition from a two-peak to one-peak DC curve simulated in [15] can be qualitatively described in terms of our model considering the suppressed maximum instead of full extinction. Let us compare the ideal flat geometry and the surface with the lowest

roughness, which are noted as S_0 and S_1 in Fig. 2(c). The surface region of S_1 is filled by the smallest ions mainly, leaving the other component at the volume region. Such asymmetry promotes only one enhanced peak corresponding to the situation when the smallest-size component is counterions. Thus, as one can see from inset in Fig. 2(c) the increase of the surface roughness transforms two comparable peaks S_0 of DC to one dominating peak S_1 .

The quantitative predictions for the concentrated ionic liquids presented above are limited by the simple mean-field approach used in the chemical potentials calculations. This model omits the effects from both electrostatic correlations [41] and an accurate hard-sphere equation of state depending on the weighted densities [43]. However, it is possible to address these shortcomings extending the proposed approach for the more sophisticated models beyond the mean-field ones, for example, the Bazant-Storey-Kornyshev (BSK) theory [32] accounting for the electrostatic correlations, and very recent work [33] showing the spatial oscillations of the ion density. Since in the BSK theory [32] the calculation of the ion chemical potentials is very similar to the model considered here [25], the rough surface results from the current work are applicable to BSK theory as well. A more recent model [33] is formulated in terms of the weighted charge densities that results in the Helmholtz free energy functional similar to FMT [43]. The random surface extension of the FMT-based functional was already investigated in the problem of uncharged molecules adsorptions [44,45]. Therefore, our approach applied to both models [32,33] can provide equations for the ion density distributions near rough surfaces, which will depend on the averaged electrostatic fields. The electrostatic properties can be defined separately, considering the corresponding differential equations with the boundary conditions on the rough (random) surfaces. In one model [33] the electrostatic field is defined by the Poisson equation with the weighted charged density in the right-hand side. Therefore, the application of the perturbation theory [35] will result in expressions

similar to those in the current work. Also, the perturbation technique [35] could be used for the modified Poisson equation from [32], that potentially will demand a higher order expansion. Thus, similarly to current work, separated rough surface modifications for the ions distribution densities and electrostatic fields will provide the self-consistent equations for models [32,33].

In future works, besides models [32,33] we will implement the rough surface approach into classical Density Functional Theory (c-DFT), which successfully describes static [41] and dynamic [46] properties of the supercapacitors. Despite several versions of c-DFT describing the adsorption of the neutral molecules on the rough uncharged surfaces [34,44,45] the electrostatic c-DFT has been previously applied to flat electrodes only. Detailed theoretical investigation of the electrolyte behavior near a rough surface could explain the difference of the roughness impact on the ionic liquids and the solutions described in [20] accounting for the the solvent molecule compatible adsorption which effectively decreases the surface roughness.

One of the interesting features of our theory is the relative character of the roughness influence. Indeed, as one can see from the model description shown here and in [44,47], the averaged properties are defined by the dimensionless parameters (δ/d_i , λ/d_i). Therefore, it is possible to investigate the roughness-induced effects considering only one surface sample and a set of cations and anions with various diameters. This scheme is similar with Parsons-Zobel plot [48] showing the dependence of the inverse value of the experimentally measured capacity $1/C_{\text{exp}}$ on the theoretically predicted one $1/C_{\text{th}}$ for the different electrolytes. Regarding the process of the experimental measurements, the impedance data of nonideal capacitors is often interpreted in terms of

a constant phase element [49]. This approach provides the power-law dependence of the capacitance on the frequency ω in the form $C \sim (\omega i)^{\alpha-1}$, where α is the system parameter $0 < \alpha \leq 1$. The experiments show that $\alpha \rightarrow 1$ as more smoother and cleaner electrodes are considered [49]. The connection between the frequency dependence of the capacity and roughness was identified long ago in [50]. Since the porous materials roughness is the multiscale characteristic, it is a complicated problem to identify the explicit origin of the observed frequency dependence. Studies [51,52] revealed that it is the atomic scale surface heterogeneities which induce the dispersion behavior. Our model accounts for such scale of the heterogeneity, which can be used to develop the rough surface dynamics model describing the ions adsorption at time-dependent potentials $U = U_0 \cos \omega t$. For example, the impedance for flat electrodes can be calculated using the dynamic density functional theory [53]. Thus, a random surface extension of the electrolyte c-DFT approach could be useful for the investigation of the capacitance dispersion.

In conclusion, we developed a theory describing the ion distribution structure and accounting for the realistic roughness of the porous electrodes. Our model predicts the significant capacitance increase induced by ions-scale roughness. Moreover, we observed that the shape of the DC dependency on applied potential changes notably with a variation of roughness and becomes sharper as the roughness increases.

T.A. acknowledges the financial support from the Russian Science Foundation (Project No. 20-72-00183). K.S. is grateful to Schlumberger management for the permission to publish this work. The authors are grateful to Mikhail Stukan for useful comments. T.A. and K.S. contributed equally to this work.

-
- [1] P. Simon and Y. Gogotsi, *Nat. Mater.* **19**, 1151 (2020).
- [2] J. Gamby, P. Taberna, P. Simon, J. Fauvarque, and M. Chesneau, *J. Power Sources* **101**, 109 (2001).
- [3] J. Chmiola, G. Yushin, R. Dash, and Y. Gogotsi, *J. Power Sources* **158**, 765 (2006).
- [4] M. Härmas, R. Palm, T. Thomberg, R. Härmas, M. Koppel, M. Paalo, I. Tallo, T. Romann, A. Jänes, and E. Lust, *J. Appl. Electrochem.* **50**, 15 (2020).
- [5] F. Béguin, V. Presser, A. Balducci, and E. Frackowiak, *Adv. Mater.* **26**, 2219 (2014).
- [6] J. Chmiola, G. Yushin, Y. Gogotsi, C. Portet, P. Simon, and P.-L. Taberna, *Science* **313**, 1760 (2006).
- [7] C. Largeot, C. Portet, J. Chmiola, P.-L. Taberna, Y. Gogotsi, and P. Simon, *J. Am. Chem. Soc.* **130**, 2730 (2008).
- [8] D.-e. Jiang, Z. Jin, and J. Wu, *Nano Lett.* **11**, 5373 (2011).
- [9] S. Kondrat and A. Kornyshev, *J. Phys.: Condens. Matter* **23**, 022201 (2010).
- [10] S. Kondrat, N. Georgi, M. V. Fedorov, and A. A. Kornyshev, *Phys. Chem. Chem. Phys.* **13**, 11359 (2011).
- [11] A. Sheehan, L. A. Jurado, S. N. Ramakrishna, A. Arcifa, A. Rossi, N. D. Spencer, and R. M. Espinosa-Marzal, *Nanoscale* **8**, 4094 (2016).
- [12] M. A. Vorotyntsev, in *Modern Aspects of Electrochemistry*, edited by B. E. Conway, J. O' M. Bockris, and R. E. White, Vol. 17 (Springer, New York, 1986), pp. 131–222.
- [13] L. I. Daikhin, A. A. Kornyshev, and M. Urbakh, *Phys. Rev. E* **53**, 6192 (1996).
- [14] L. Daikhin, A. Kornyshev, and M. Urbakh, *J. Chem. Phys.* **108**, 1715 (1998).
- [15] J. Vatamanu, L. Cao, O. Borodin, D. Bedrov, and G. D. Smith, *J. Phys. Chem. Lett.* **2**, 2267 (2011).
- [16] L. Xing, J. Vatamanu, G. D. Smith, and D. Bedrov, *J. Phys. Chem. Lett.* **3**, 1124 (2012).
- [17] Z. Hu, J. Vatamanu, O. Borodin, and D. Bedrov, *Phys. Chem. Chem. Phys.* **15**, 14234 (2013).
- [18] J. Vatamanu, L. Xing, W. Li, and D. Bedrov, *Phys. Chem. Chem. Phys.* **16**, 5174 (2014).
- [19] D. Bedrov, J. Vatamanu, and Z. Hu, *J. Non-Cryst. Solids* **407**, 339 (2015).
- [20] J. Vatamanu, O. Borodin, M. Olguin, G. Yushin, and D. Bedrov, *J. Mater. Chem. A* **5**, 21049 (2017).
- [21] J. Wei, Y. Li, D. Dai, F. Zhang, H. Zou, X. Yang, Y. Ji, B. Li, and X. Wei, *ACS Appl. Mater. Interfaces* **12**, 5786 (2020).
- [22] J. Vatamanu, M. Vatamanu, and D. Bedrov, *ACS nano* **9**, 5999 (2015).

- [23] Y.-Z. Su, Y.-C. Fu, J.-W. Yan, Z.-B. Chen, and B.-W. Mao, *Angew. Chem. Intl. Ed.* **48**, 5148 (2009).
- [24] Y. Lauw, M. D. Horne, T. Rodopoulos, V. Lockett, B. Akgun, W. A. Hamilton, and A. R. Nelson, *Langmuir* **28**, 7374 (2012).
- [25] A. A. Kornyshev, *J. Phys. Chem. B* **111**, 5545 (2007).
- [26] Z. A. Goodwin, G. Feng, and A. A. Kornyshev, *Electrochim. Acta* **225**, 190 (2017).
- [27] G. Feng, M. Chen, S. Bi, Z. A. H. Goodwin, E. B. Postnikov, N. Brilliantov, M. Urbakh, and A. A. Kornyshev, *Phys. Rev. X* **9**, 021024 (2019).
- [28] A. Gupta, A. Govind Rajan, E. A. Carter, and H. A. Stone, *Phys. Rev. Lett.* **125**, 188004 (2020).
- [29] H. Chao and Z.-G. Wang, *J. Phys. Chem. Lett.* **11**, 1767 (2020).
- [30] M. Janssen, *Phys. Rev. E* **100**, 042602 (2019).
- [31] M. V. Fedorov and A. A. Kornyshev, *Chem. Rev.* **114**, 2978 (2014).
- [32] M. Z. Bazant, B. D. Storey, and A. A. Kornyshev, *Phys. Rev. Lett.* **106**, 046102 (2011).
- [33] J. P. de Souza, Z. A. H. Goodwin, M. McEldrew, A. A. Kornyshev, and M. Z. Bazant, *Phys. Rev. Lett.* **125**, 116001 (2020).
- [34] A. V. Neimark, Y. Lin, P. I. Ravikovitch, and M. Thommes, *Carbon* **47**, 1617 (2009).
- [35] M. Dambrine, I. Greff, H. Harbrecht, and B. Puig, *SIAM J. Numer. Anal.* **54**, 921 (2016).
- [36] C. Ciraci, F. Vidal-Codina, D. Yoo, J. Peraire, S.-H. Oh, and D. R. Smith, *ACS Photonics* **7**, 908 (2020).
- [37] E. Gadelmawla, M. Koura, T. Maksoud, I. Elewa, and H. Soliman, *J. Mater. Process. Technol.* **123**, 133 (2002).
- [38] X. Wang, M. Salari, D.-e. Jiang, J. C. Varela, B. Anasori, D. J. Wesolowski, S. Dai, M. W. Grinstaff, and Y. Gogotsi, *Nat. Rev. Mater.* **5**, 787 (2020).
- [39] S. Evlashin, F. Fedorov, P. Dyakonov, Y. M. Maksimov, A. Pilevsky, K. Maslakov, Y. O. Kuzminova, Y. A. Mankelevich, E. Voronina, S. Dagesyan *et al.*, *J. Phys. Chem. Lett.* **11**, 4859 (2020).
- [40] See Supplemental Material at <http://link.aps.org/supplemental/10.1103/PhysRevE.103.L060102>, which includes Refs. [54–56], for derivation of equations governing electrostatic field and average distributions of ions near rough surface, random surface model and hard sphere contact condition, and notes on numerical implementation.
- [41] A. Härtel, *J. Phys.: Condens. Matter* **29**, 423002 (2017).
- [42] M. V. Fedorov and A. A. Kornyshev, *J. Phys. Chem. B* **112**, 11868 (2008).
- [43] R. Roth, *J. Phys.: Condens. Matter* **22**, 063102 (2010).
- [44] T. Aslyamov and A. Khlyupin, *J. Chem. Phys.* **147**, 154703 (2017).
- [45] T. Aslyamov, V. Pletneva, and A. Khlyupin, *J. Chem. Phys.* **150**, 054703 (2019).
- [46] T. Aslyamov, K. Sinkov, and I. Akhatov, [arXiv:2011.04575](https://arxiv.org/abs/2011.04575) (2020).
- [47] A. Khlyupin and T. Aslyamov, *J. Stat. Phys.* **167**, 1519 (2017).
- [48] R. Parsons and F. R. Zobel, *J. Electroanal. Chem.* (1959) **9**, 333 (1965).
- [49] V. Lockett, R. Sedev, J. Ralston, M. Horne, and T. Rodopoulos, *J. Phys. Chem. C* **112**, 7486 (2008).
- [50] T. Borisova and B. Ershler, *Zh. Fiz. Khim* **24**, 337 (1950).
- [51] Z. Kerner and T. Pajkossy, *J. Electroanal. Chem.* **448**, 139 (1998).
- [52] Z. Kerner and T. Pajkossy, *Electrochim. Acta* **46**, 207 (2000).
- [53] S. Babel, M. Eikerling, and H. Löwen, *J. Phys. Chem. C* **122**, 21724 (2018).
- [54] G. Caloz, M. Costabel, M. Dauge, and G. Vial, *Asymptotic Anal.* **50**, 121 (2006).
- [55] T. Aslyamov and I. Akhatov, *Phys. Rev. E* **100**, 052118 (2019).
- [56] Wolfram Research, Inc., *Mathematica*, Version 12.1 (Champaign, IL, 2020).